Molecular Crystals and Liquid Crystals

ISSN: 1542-1406 (Print) 1563-5287 (Online) Journal homepage: http://www.tandfonline.com/loi/gmcl20

Kinetics of mullite formation from kaolinite and boehmite

M. Heraiz, F. Sahnoune, M. Hrairi, N. Saheb & A. Ouali

To cite this article: M. Heraiz, F. Sahnoune, M. Hrairi, N. Saheb & A. Ouali (2016) Kinetics of mullite formation from kaolinite and boehmite, Molecular Crystals and Liquid Crystals, 628:1, 55-64, DOI: 10.1080/15421406.2015.1137113

To link to this article: http://dx.doi.org/10.1080/15421406.2015.1137113

Published online: 13 May 2016.

MOL. CRYST. LIQ. CRYST.
2016, VOL. 628, 55–64
http://dx.doi.org/10.1080/15421406.2015.1137113

Taylor & Francis
Taylor & Francis Group

Kinetics of mullite formation from kaolinite and boehmite

M. Heraiz[a], F. Sahnoune[a], M. Hrairi[b], N. Saheb[c], and A. Ouali[a]

[a]Physics and Chemistry of Materials Lab, University of M'sila, M'sila, Algeria; [b]Departments of Mechanical Engineering, Faculty of Engineering, International Islamic University Malaysia, Kuala Lumpur, Malaysia; [c]Departments of Mechanical Engineering, King Fahd University of Petroleum and Minerals, Dhahran, Saudi Arabia

ABSTRACT

The excellent electrical, thermal and mechanical properties, and good stability of mullite made it a candidate material to produce ceramics for advanced applications such as catalyst supports, filters, optical devices, heat exchangers and electronic packaging. In this work, monolithic mullite was synthesized from kaolinite and boehmite and the kinetics of its formation was investigated using dilamometry. The activation energies for the transformation of kaolinite to metakaolinite, transformation of metakaolinite to spinel, and transformation of the kaolinite-boehmite powder to mullite were evaluated through non-isothermal treatment following the Kissinger and Ozawa equations. The growth morphology parameters were evaluated for the transformation of metakaolinite to spinel, and for the transformation of the spinel to mullite.

KEY WORDS

Mullite; Kaolinite; Boehmite; Dilamometry; Activation energy; Avrami parameter

Introduction

Mullite ($3Al_2O_3{\cdot}2SiO_2$), a stable compound in the SiO_2–Al_2O_3 system, is one of the most important phases found in traditional and technical ceramics [1]. Its excellent electrical, thermal and mechanical properties, and good stability made it a candidate material to produce ceramics for advanced applications such as catalyst supports, filters, optical devices, heat exchangers and electronic packaging [2–4]. Many methods were used to synthesize monolithic mullite or materials based on mullite [1, 5–11]. One way to synthesize mullite is through firing kaolinite and boehmite. Kaolinite [$Al_2Si_2O_5(OH)_4$], is a layer silicate in the form of micro-crystals with a crystal structure consisting of a single silica tetrahedral sheet and a single alumina octahedral sheet [5]. Boehmite [12, 13] a partially dehydrated aluminum hydroxide, can be produced from aluminum hydroxides by controlled calcinations [14–16]. Also, thermal calcination in air can convert gibbsite to boehmite [17, 18] which is frequently used as starting material for the synthesis of alumina phases [12, 13]. In previous works, the authors synthesized mullite through reaction sintering kaolinite with pure alumina [19], analyzed the kinetics of the dehydroxylation of kaolinite through thermal analysis [20]; and investigated the kinetics of mullite formation from kaolinite and pure alumina; and evaluated the temperature of formation, activation energies and growth morphology parameters [21]. Also, the authors synthesized Al_2O_3 containing mullite from kaolinite and boehmite [9], and characterized its microstructure and properties. The objective of the present work is to investigate the kinetics of monolithic mullite formation from kaolinite and boehmite through non-isothermal

CONTACT M. Heraiz heraizme@yahoo.fr Physics and Chemistry of Materials Lab, University of M'sila, M'sila, Algeria

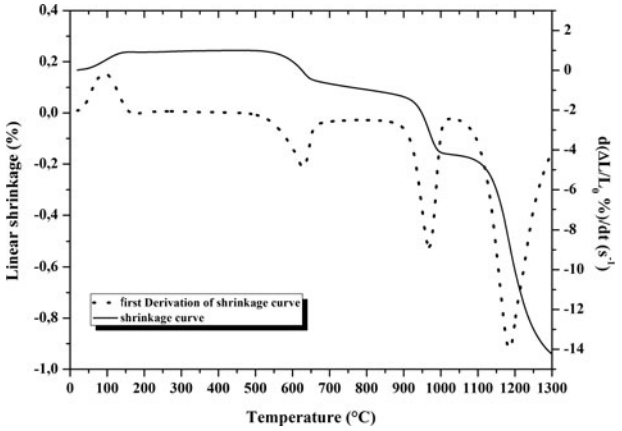

Figure 1. Linear shrinkage curve and its first derivative for kaolinite-boehmite mixture treated at heating rate of 10°C/min.

treatment using dilatometry and evaluate the activation energy and Avrami parameter for the different transformations that lead to the formation of mullite.

Materials and procedures

Comprehensive information and chemical composition of the kaolinite and Boehmite used in this investigation were provided elsewhere [9]. A homogeneous mixture of kaolinite and boehmite was prepared using ball milling technique. The boehmite was added to the kaolinite according to the stoichiometry that only leads to the formation of mullite ($3Al_2O_3.2SiO_2$). Zirconia vials and balls with ball-to-powder weight ratio of 10:1 were used. Water was added to the kaolinite and boehmite mixture at a ratio of 2:1. The mixture was milled at room temperature, at a rotation speed of 250 rpm for 5 hours, in a high-energy planetary ball mill (Fritsch P6). The milled mixture was dried at 100°C for 6 hours then cold compacted at 75 MPa using uniaxial press to produce specimens of 13 mm diameter. Dilatometry experiments were performed on samples using a NETZSCH (Dil 402 C) dilatometer. The samples were heated from room temperature to 1300°C, at heating rates of 5, 10 and 20°C/min. Details on the analysis of the isothermal and non-isothermal treatments were reported elsewhere [20, 21] according to procedures followed in [22–23] and are used in this work to evaluate the activation energies and growth parameters.

Results and discussion

Figure 1 shows a typical linear shrinkage curve and its first derivative for kaolinite-boehmite mixture treated at heating rate of 10°C/min. It can be clearly seen that there are four transformations. The first transformation is a relative linear expansion at a temperature lower than 160°C due to the dehydroxylation of the raw kaolin and the formation of kaolinite where the rate is maximum at 94°C. The second transformation is a relative linear shrinkage which starts at 500°C and ends at 670°C where the rate of shrinkage is maximum at 628°C; this shrinkage is due to the evaporation of water in the kaolinite which transforms to metakaolinite. The third transformation is a second relative linear shrinkage that corresponds to the change of metakaolinite to spinel (Al-Si) and a none-crystalline SiO_2 and the rate of transformation is

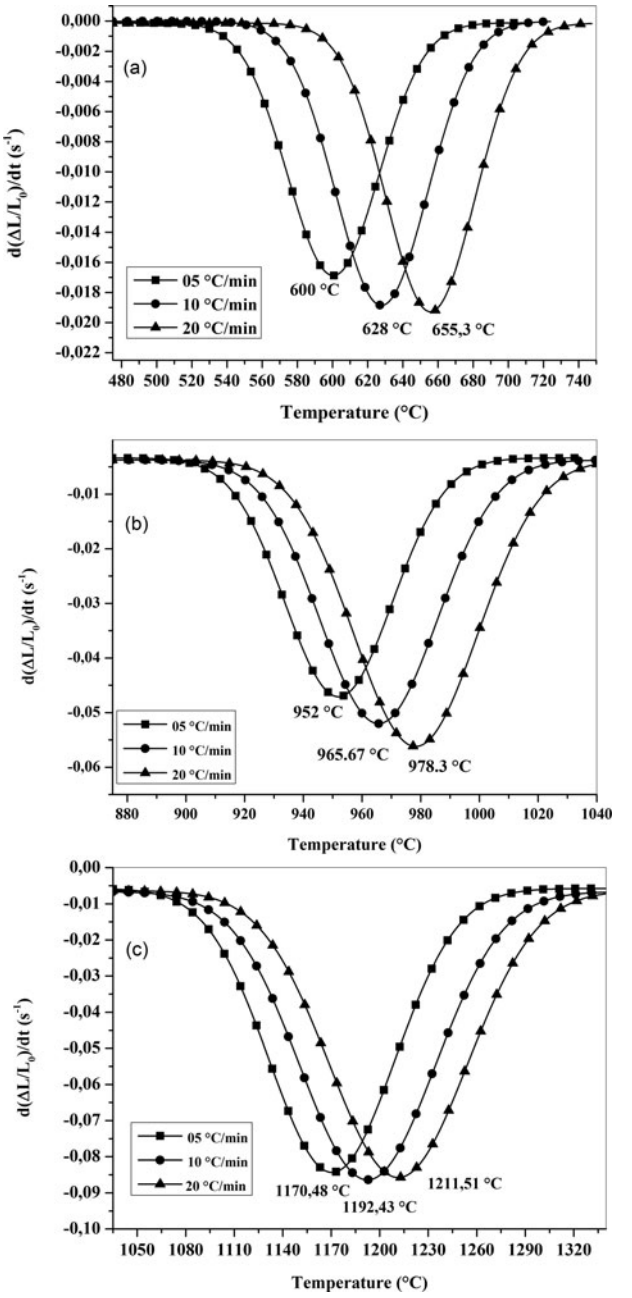

Figure 2. First derivative shrinkage curves for the transformation of (a) kaolinite to metakaolinite, (b) metakaolinite to spinel, (c) spinel to mullite, in kaolinite-boehmite mixture.

maximum at 965°C. The fourth transformation is a third relative linear shrinkage that corresponds to the change of spinel to silica in the form of cristobalite and primary mullite at a temperature of 1192°C and this transformation ends at a temperature lower that 1300°C. Similar linear shrinkage curves were recorded at heating rates of 5 and 20°C/min.

The linear relative shrinkage curves as function of temperature at heating rates of 5, 10, and 20°C/min were used to calculate the activation energy for the formation of the different phases following the Kissinger and Ozawa equations. The maximum temperature (T_m), at different

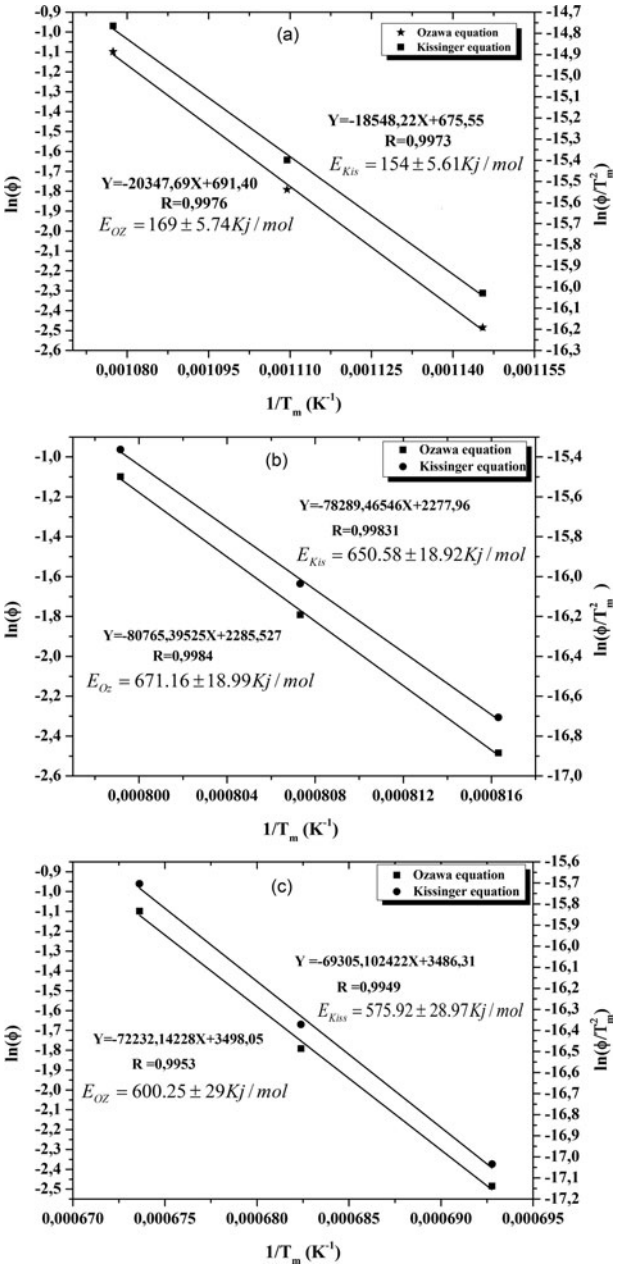

Figure 3. Plots of $\ln(\phi)$ and $\ln(\phi/T_m^2)$ versus $1/T_m$ for the transformation of (a) kaolinite to metakaolinite, (b) metakaolinite to spinel, (c) spinel to mullite, in kaolinite-boehmite mixture.

heating rates, for the transformation of kaolinite to metakaolinite, figure 2(a), metakaolinite to spinel, figure 2(b), and spinel to mullite, figure 2(c), was obtained from the derivative of the linear shrinkage curves.

Figure 3(a) shows change of $\ln(\phi/T_m^2)$ and $\ln(\phi)$ as function of the inverse of temperature $1/T_m$ for the transformation of kaolinite to metakaolinite. The values of the activation energy for the formation of metakaolinite are 154 kJ/mol and 169 kJ/mol following the Kissinger and Ozawa equations, respectively. The obtained values are close to 177.75 kJ/mol reported by Sahnoune and co-workers [20] using deferential thermal analysis (DTA). Figure 3(b) shows

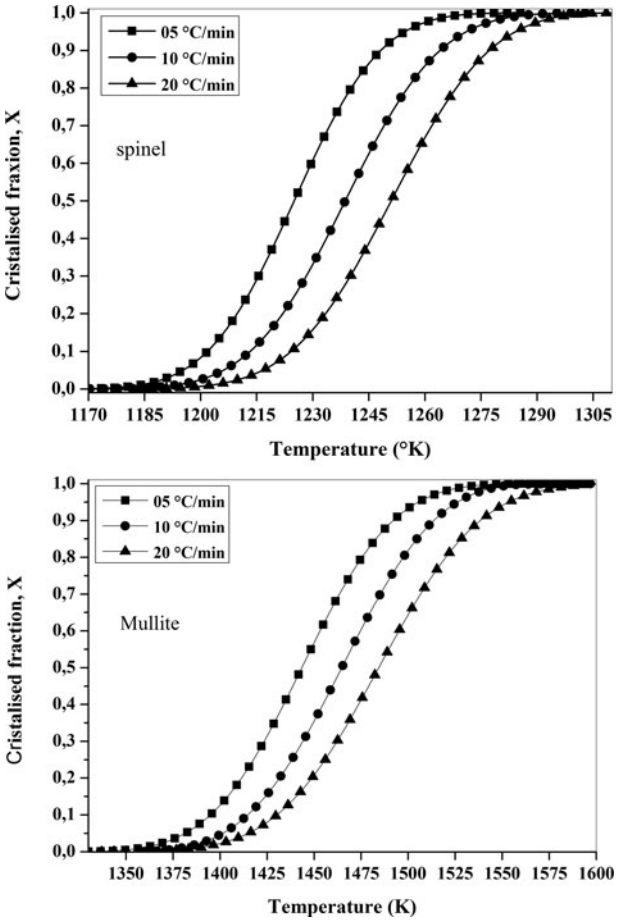

Figure 4. Variation of crystallised fraction of (a) spinel and (b) mullite, with temperature for kaolinite-boehmite mixture under different heating rates.

change of $\ln(\phi/T_m^2)$ and $\ln(\phi)$ as function of the inverse of temperature $1/T_m$ for the transformation of metakaolinite to spinel. The values of the activation energy for the formation of spinel are 650 ± 18.92 kJ/mol and 671.16 ± 18.99 kJ/mol following the Kissinger and Ozawa equations, respectively. Figure 3(c) shows change of $\ln(\phi/T_m^2)$ and $\ln(\phi)$ as function of the inverse of temperature $1/T_m$ for the transformation of spinel to mullite. The values of the activation energy for the formation of mullite are 575.92 ± 28.97 kJ/mol and 600.25 ± 29 kJ/mol following the Kissinger and Ozawa equations, respectively.

The activation energy for mullite formation were reported by many others [21, 24–26]. Gualtieri [24] reported activation energy of 523 kJ/mol for mullite formation from kaolinite. Romero et al. [22] investigated the growth of mullite in a porcelain stoneware body and reported non-isothermal activation energy of 622 kJ/mol, Vieira and Ramos investigated mullitisation kinetics from silica and alumina rich wastes [26] using differential dilatometry; they reported non-isothermal activation energies of 431 and 454 kJ/mol for formation of primary and secondary mullite, respectively. The discrepancies between the reported activation energies and growth morphology parameters for mullite formation were attributed to the different types of raw materials used for mullite synthesis in addition to the different chemical composition and/or particle size distribution.

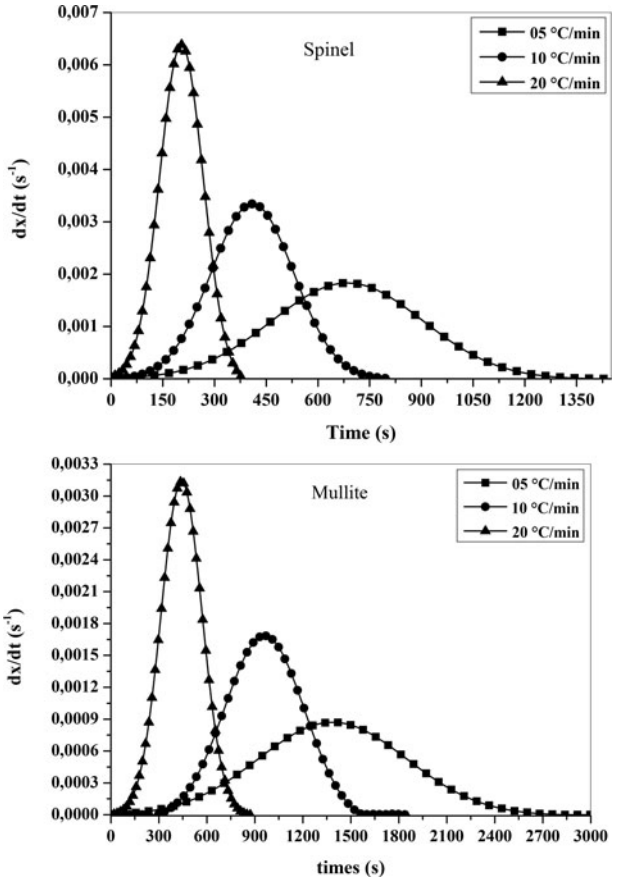

Figure 5. Growth rate of (a) spinel and (b) mullite with time for kaolinite-boehmite powder at different heating rates.

The variation of crystallised fraction of spinel and mullite with temperature under different heating rates is presented in figure 4. The crystallised fraction, x, was determined from dilatometry results as:

$$X = A_T/A_0$$

where A_T is the area of the peak in the dilatometry curve at temperature T, and A_0 is the total area under the peak. The crystallised fraction, x, at a temperature T differs at different heating rates and hence the curves of dx/dt versus time are also different as shown in figure 5, which depicts the growth rate of spinel and mullite with time at different heating rates. The rate of crystallisation increases with the increase in heating rate.

Figure 6 shows the plot of ln(dx/dt) versus 1/T at the same value of crystallised fraction, x, from the experiments at different heating rates as proposed by Ligero et al [23]. The values of the activation energy, E, for different crystallised fraction, which were calculated by the average of the slopes of the lines, are presented in Table 1.The values of the activation energy are 626.98 kJ/mol and 561.56 kJ/mol for the formation of spinel and mullite, respectively.

Figure 7 shows the plot of $\ln\{k_0 f(x)\}$ versus crystallised fraction, X, for a kaolinite-behomite powder heated at a heating rate of 5°C/min. The Avrami parameter, n, was determined by the selection of many pairs of X1, and X2 that satisfied the condition $\ln\{k_0 f(x1)\} = \ln\{k_0 f(x2)\}$. The average values of n for each heating rate are presented in table 2. The average Avrami

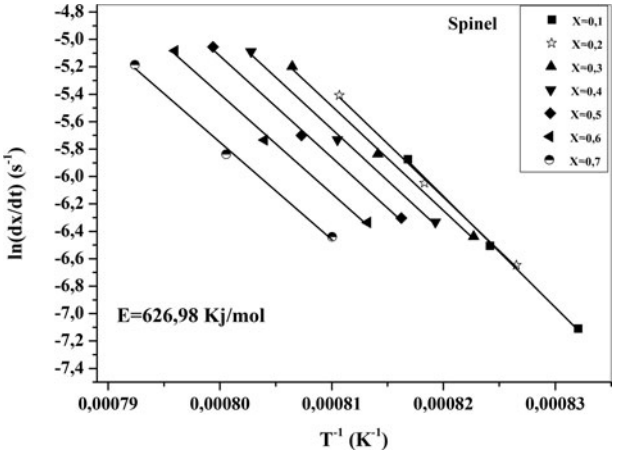

Figure 6. Plot of ln(d*x*/d*t*) versus 1/*T* at the same value of crystallised fraction, *x*, from the experiments at different heating rates for (a) spinel, (b) mullite.

parameter is 1.30 for spinel formation and 1.16 for mullite formation. These values are close to 1.5 for spinel formation and 1 for mullite formation, which suggests that the crystallisation process, in kaolin-boehmite powder, is controlled by diffusion growth for spinel formation and by interface reaction for mullite formation [22].

Sahnoune and co-workers [21] analyzed mullite formation from Algerian kaolinite using DTA and reported an activation energy of around 1260 kJ/mol measured from non-isothermal treatment, also, they reported a growth morphology parameter of 1.5. Chen and co-workers [26] in their investigation on phase transformation and growth of mullite in kaolin ceramics reported that the non-isothermal activation energy of mullite crystallisation was 1182.3 kJ/mol, the growth morphology parameter n was 1.5 and the activation energy for secondary mullite formation was 454.6 kJ/mol^{-1} [27.28].

Table 1. Values of the activation energy, E, for different crystallised fraction.

	Formation of spinel		Formation of mullite	
X	R^2	E(KJmol^{-1})	R^2	E(KJmol^{-1})
0.1	0,9978	673,68	0,9982	592.30
0.2	0,9967	649,78	0,9986	578.72
0.3	0,9954	634,00	0,99869	572.16
0.4	0,9939	625,38	0,9993	563.15
0.5	0,9938	614,61	0,9997	557.33
0.6	0,9917	601,99	0,9999	551.23
0.7	0,9916	589,42	0,9991	546.6
0.8	0,9856	586,81	0,995	530.97
0.9	0,984	580,20	0,8798	518.85

Table 2. Values of the Avrami parameter, n, for different heating rate.

Heating rate (°C/min)	Spinel n	Mullite n
05	1.34	1.15
10	1.29	1.15
20	1.27	1.17

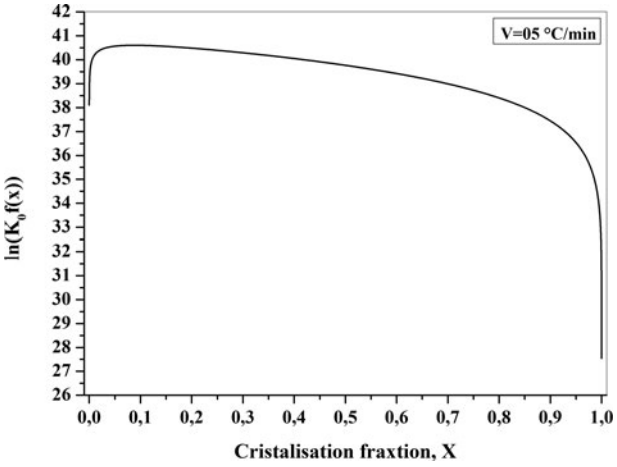

Figure 7. Plot of $\ln[k_0 f(x)]$ versus crystallised fraction, x, for a kaolinite-boehmite powder heated at a heating rate of 05°C/min.

Figure 8 shows the plots of $\ln(\phi/T_m^2)$ and $\ln(\phi^n/T_m^2)$ versus $1/T_m$ according to Kissinger and Matusita equations [22, 29], respectively. The activation energy calculated from the slope of the Kissinger plot is 650.58 kJ/mol for spinel formation, and 575.92 kJ/mol for mullite formation, which is in good agreement with those of 626.98 and 561.56 kJ/mol, for spinel and

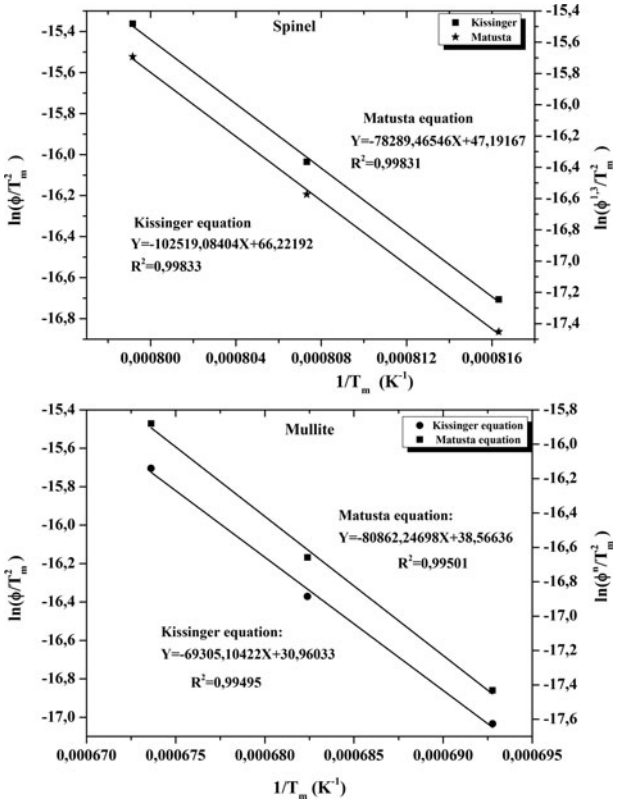

Figure 8. Plots of $\ln(\phi/T_m^2)$ and $\ln(\phi^n/T_m^2)$ versus $1/T_m$, according to Kissinger and Matusita equations, respectively, for (a) spinel, (b) mullite.

mullite formation, respectively, estimated by the Ligero method. According to Matusita equation, the parameter m was found to be 1.31 for spinel and 1.17 for mullite formation in kaolin-boehmite powder. The parameters *n* and *m* are both close to 1.5 for spinel and 1 for mullite, indicating a three-dimensional growth of spinel and mullite crystals.

Conclusion

Monolithic mullite was synthesized from kaolinite and boehmite and the kinetics of its formation was investigated. The values of the activation energy for the transformation of kaolinite to metakaolinite were found to be 154 and 169 kJ/mol following the Kissinger and Ozawa equations, respectively.

The same values were 650.58 and 671 kJ/mol for the transformation of metakaolinite to spinel, and 577.92 and 600.25 kJ/mol for the formation of mullite.

The activation energy calculated by isothermal treatment is 626.98 $\pm$ 32 kJ/mol, for the transformation of metakaolinite to spinel, and 561.56 $\pm$ 12.8 kJ/mol for the formation of mullite.

The growth morphology parameters *n* and *m* are both found to be equal to 1.3 for the transformation of metakaolinite to spinel, and 1.16 for the formation of mullite. These values are close to 1.5 for spinel formation, and 1 for mullite formation, which suggests, that the crystallisation process is controlled by diffusion growth for spinel and interface reaction for mullite.

References

[1] Santana, L. N. L., Gomes, J., Neves, G. A., Lira, H. L., Menezes, R. R., & Segadães, A. M. (2014). *Applied Clay Science*, *87*, 28–33.
[2] Carty, W. M., & Senapati, U. (2005). *J. Am. Ceram. Soc.*, *81*, 3–20.
[3] Schneider, H., Schreuer, J., & Hildmann, B. (2008). *J. Eur. Ceram. Soc.*, *28*, 329–344.
[4] Somiya, S., & Hirata, Y. (1991). *Am. Ceram. Soc. Bull.*, *70*, 1624–1632.
[5] Shoval, S., Panczer, G., & Boudeulle, M. (2008). *Optical Materials*, *30*(11), 1699–1705.
[6] Shoval, S., Boudeulle, M., & Panczer, G. (2011). *Optical Materials*, *34*(2), 404–409.
[7] Hamedani Golshan, N., Eftekhari Yekta, B., & Marghussian, V. K. (2012). *Optical Materials*, *34*(4), 596–599.
[8] Sutardi, S., Septawendar, R., & Rachman, A. (2013). *Journal of Ceramic Processing Research*, *14*(3), 400–404.
[9] Heraiz, M., Sahnoune, F., Belhouchet, H., & Saheb, N. (2013). *Journal of Optoelectronics and Advanced Materials*, 15(11–12), 1263–1267.
[10] Viswabaskaran, V., Gnanam, F. D., & Balasubramanian, M. (2003). *J. Mater. Proce. Technol.*, *142*, 275–281.
[11] Sainz, M. A., Serrano, F. J., Bastida, J., & Caballero, A. (1997). *J. Eur. Ceram. Soc.*, *17*, 1277–1284.
[12] Wang, J. Q., Liu, J. L., Liu, X. Y., Qiao, M. H., Pei, Y., & Fan, K. N. (2009). *Sci. Adv. Mater.*, *1*, 77–85.
[13] Rajabi, L., & Derakhshan, A. A. (2010). *Sci. Adv. Mater.*, *2*, 163–172.
[14] Day, M. K. B., & Hill, V. J. (1953). *J. Phys. Kolloid. Chem.*, *57*(9), 946–950.
[15] Candela, L., & Perlmutter, D. D. (1986). *AIChE J.*, *32*, 1532–1545.
[16] Candela, L., & Perlmutter, D. D. (1992). *Ind. Eng. Chem. Res.*, *31*, 694–700.
[17] Digne, M., Sautet, P., Raybaud, P., Toulhoat, H., & Artacho, E. (2002). *J. Phys. Chem. B*, *106*, 5155.
[18] Cesteros, Y., Salagre, P., Medina, F., & Sueiras, J. E. (1999). *Chem. Mater.*, *11*, 123.
[19] Sahnoune, F., Chegaar, M., Saheb, N., Goeuriot, P., & Valdivieso, F. (2008). *Appl. Clay Sci.*, *38*, 304–310.
[20] Sahnoune, F., Saheb, N., Kamal, B., & Takok, Z. (2012). *J. Therm. Anal. Calorim.*, *107*(3), 1067–1072.

[21] Sahnoune, F., Chegaar, M., Saheb, N., Gueuriot, P., & Valdivieso, F. (2008). *Advances in Applied Ceramics*, *107*(1), 9–13.
[22] Romero, M., Martín-Márquez, J., & Rincón, J. Ma. (2006). *J. Eur. Ceram. Soc*., *26*, 1647–1652.
[23] Ligero, R. A., Vazques, J., Casas-Ruiz, M., & Jimenez-Garay, R. (1991). *J. Mater. Sci*., *26*, 211–215.
[24] Gualtieri, A., Bellotto, M., Artioli, G., & Clark, S. M. (1995). *Phys. Chem. Miner*., *22*, 215–222.
[25] Vieira, S. C., Ramos, A. S., & Vieira, M. T. (2007). *Ceram. Int*., *33*, 59–66.
[26] Chen, Y. F., Wang, M. C., & Hon, M. H. (2004). *J. Eur. Ceram. Soc*., *24*, 2389–2397.
[27] Chen, Y. F., Wang, M. C., & Chang, Y. H. (2004). *Scr. Mater*., *51*, 231–235.
[28] Ptáček, P., Křečková, M., Šoukal, F., & Opravil, T. (2012). *Powder Technology*, *232*, 24–30.
[29] Matusita, K., Sakka, S., & Matsui, Y. (1975). *J. Mater. Sci*., *10*, 961–966.